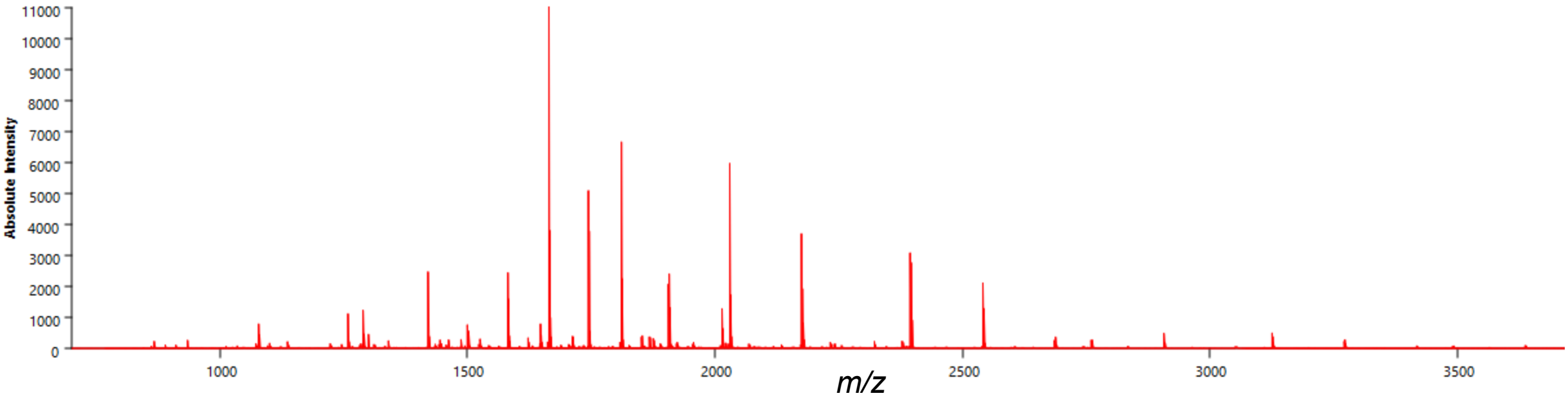
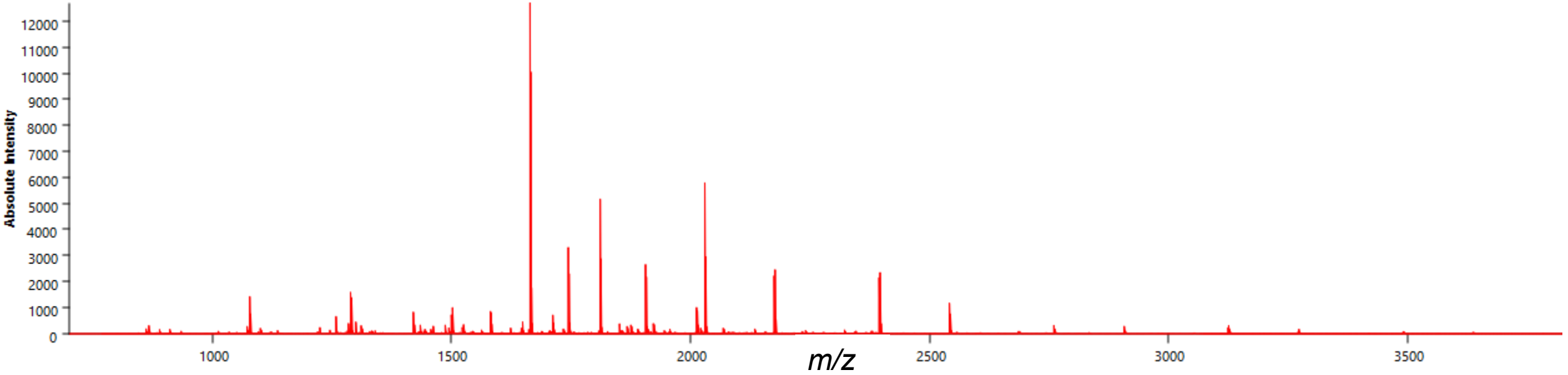


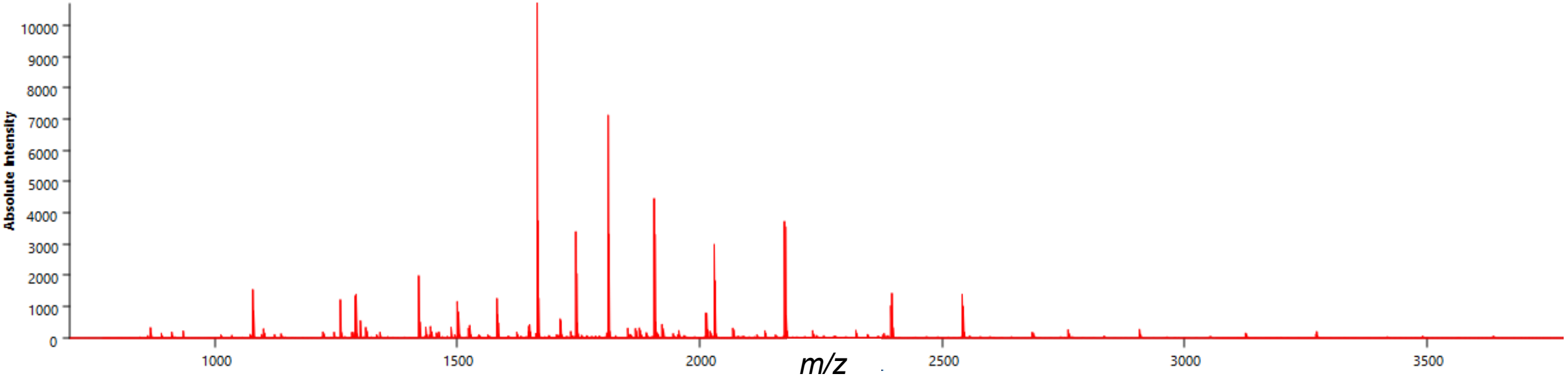
Supplemental Figure 1.

Mass spectrum showing the glycan distribution of patient PT-39



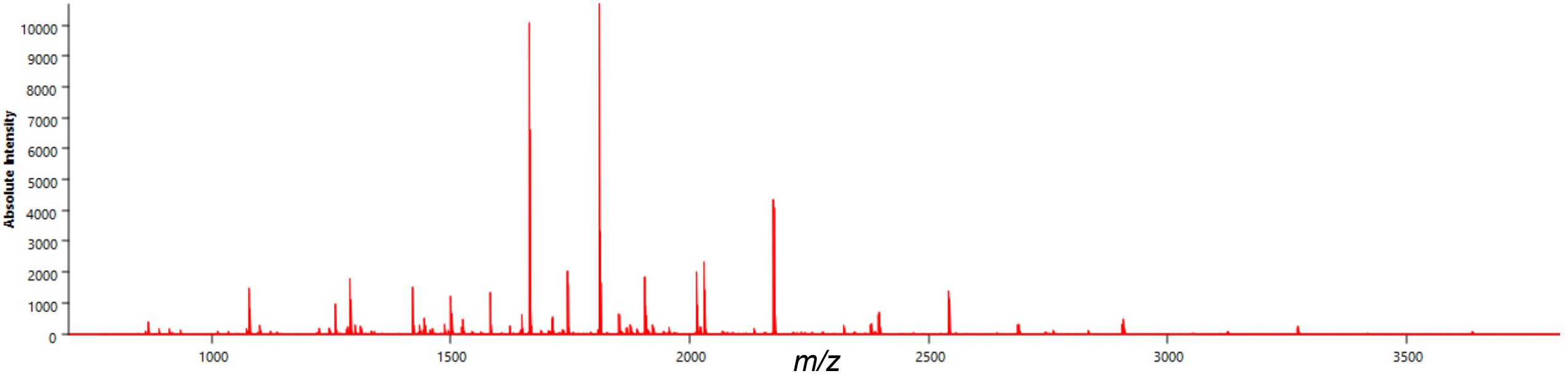
Supplemental Figure 2.

Mass spectrum showing the glycan distribution of patient PT-66



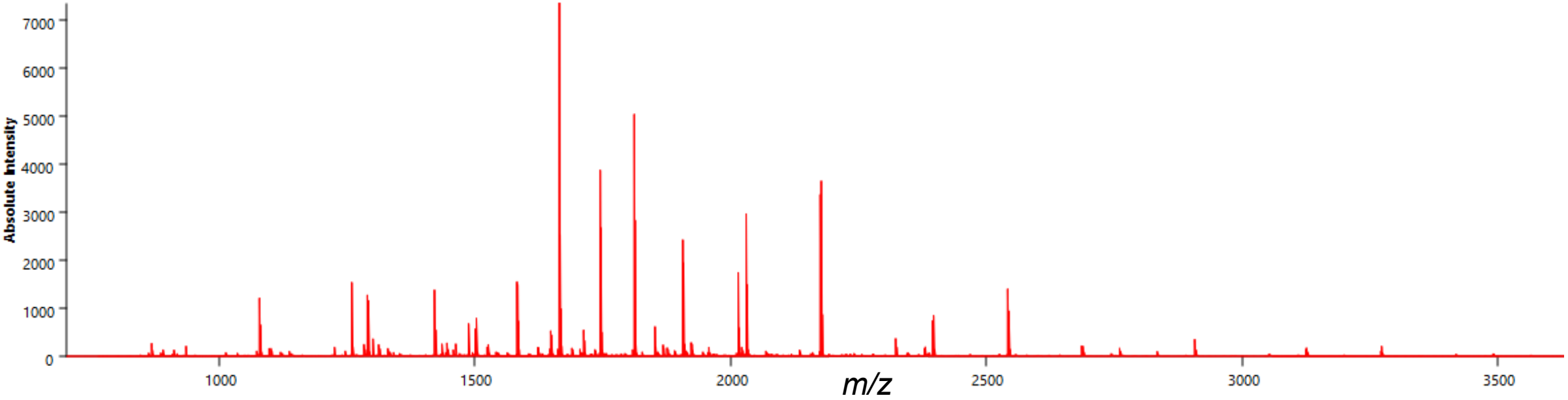
Supplemental Figure 3.

Mass spectrum showing the glycan distribution of patient PT-63



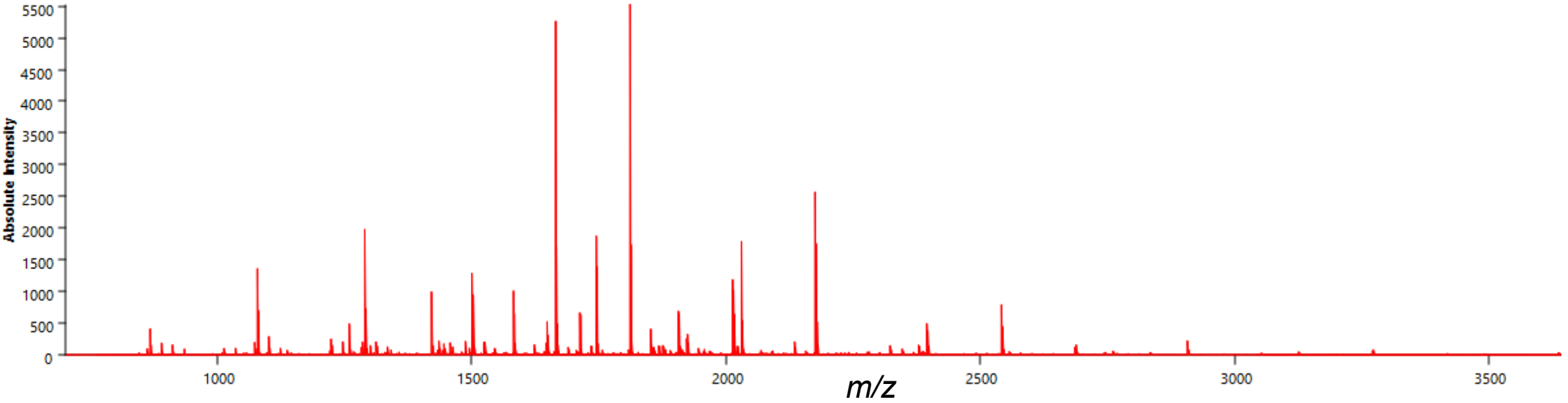
Supplemental Figure 4.

Mass spectrum showing the glycan distribution of patient PT-9



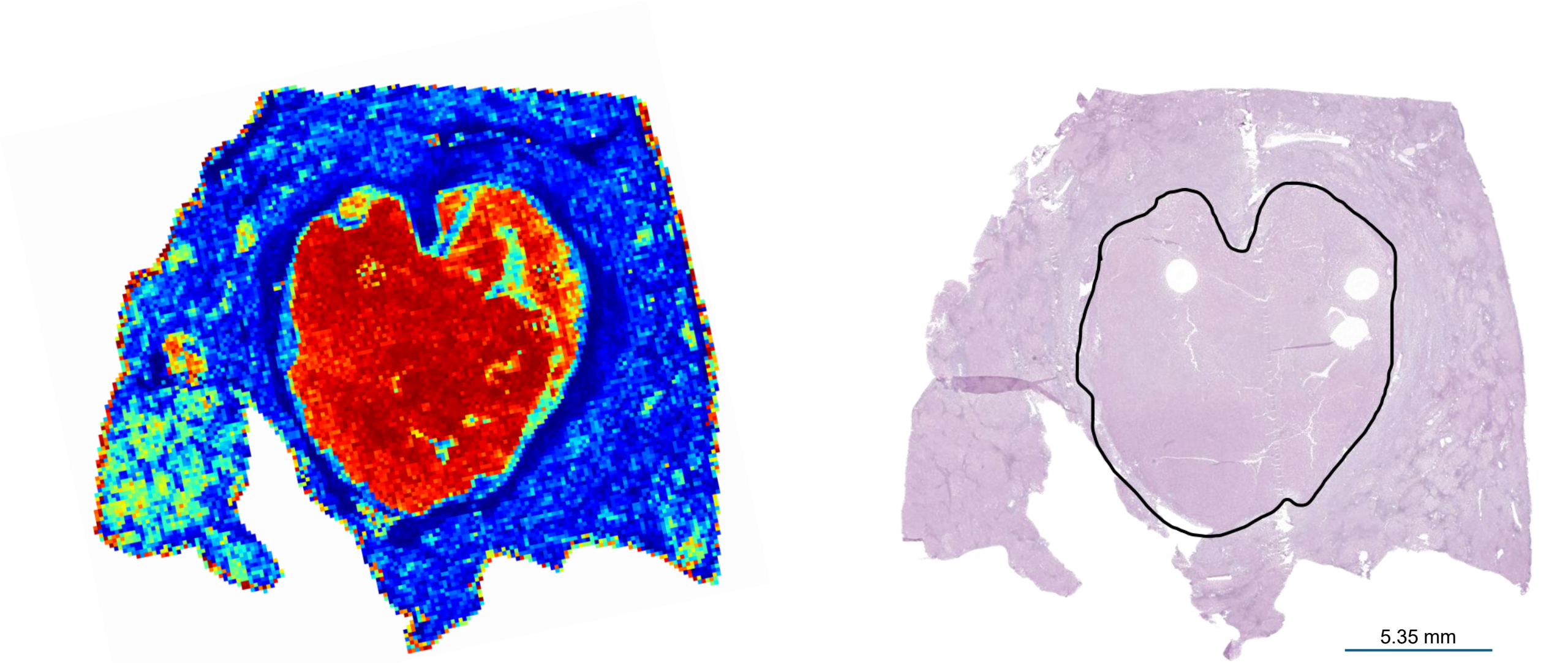
Supplemental Figure 5.

Mass spectrum showing the glycan distribution of patient PT-43



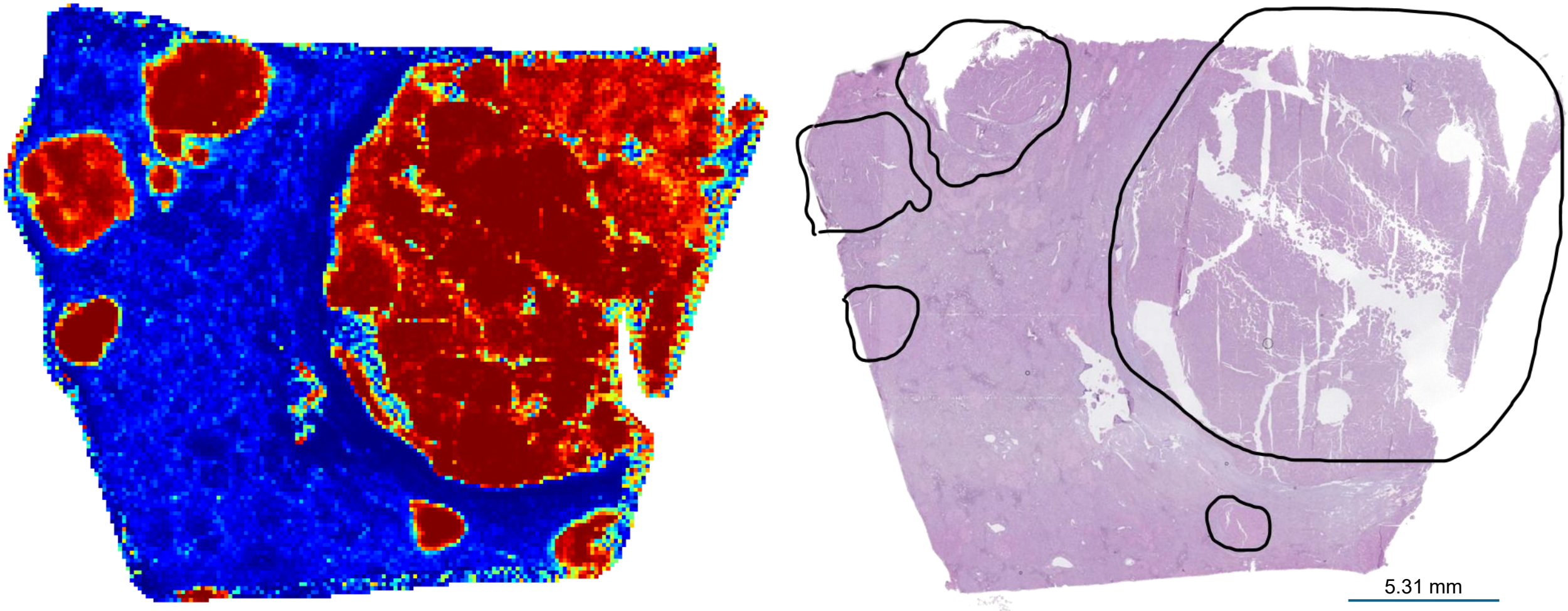
Supplemental Figure 6.

Mass spectrum showing the glycan distribution of patient PT-30



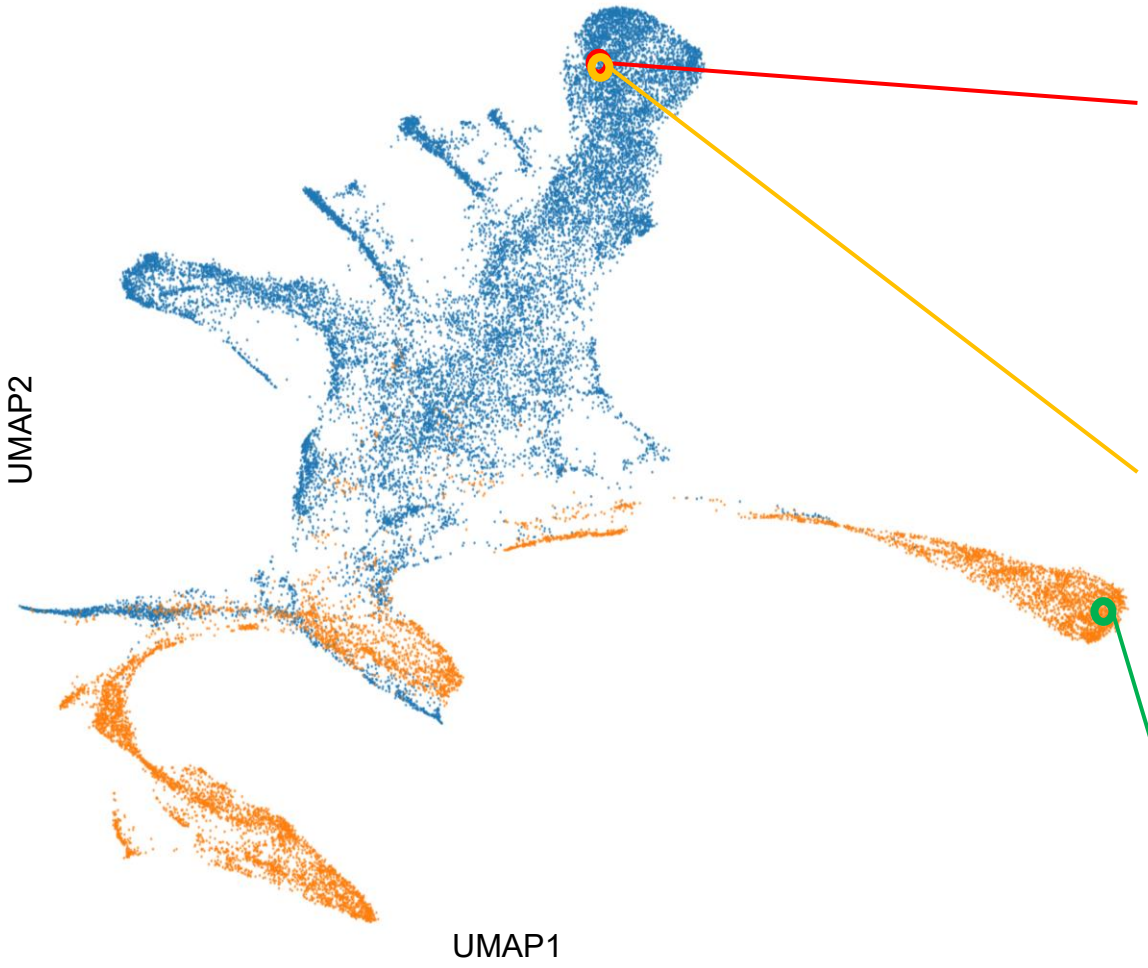
Supplemental Figure 7.

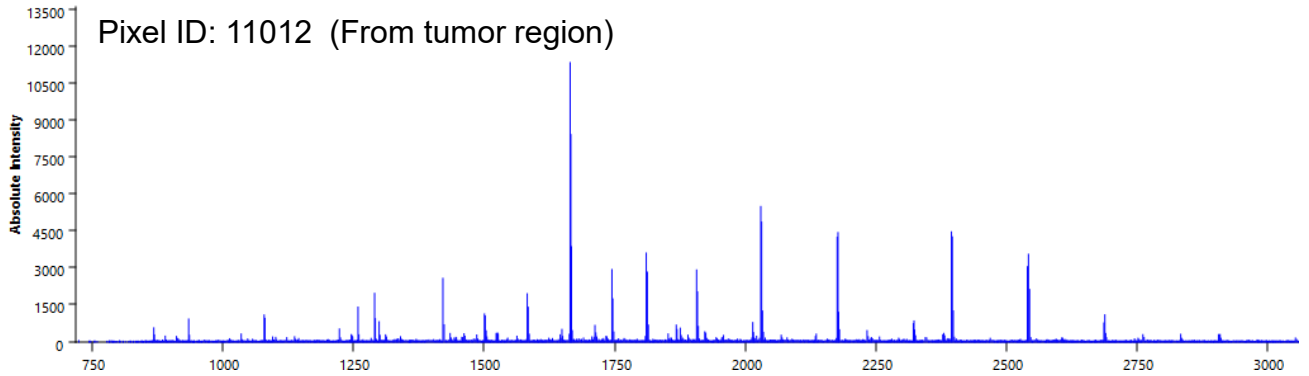
A representative sample (PT-115) demonstrating the agreement between the XGBoost-predicted tumor region (red, left) and the pathologist-annotated tumor region (black, right).

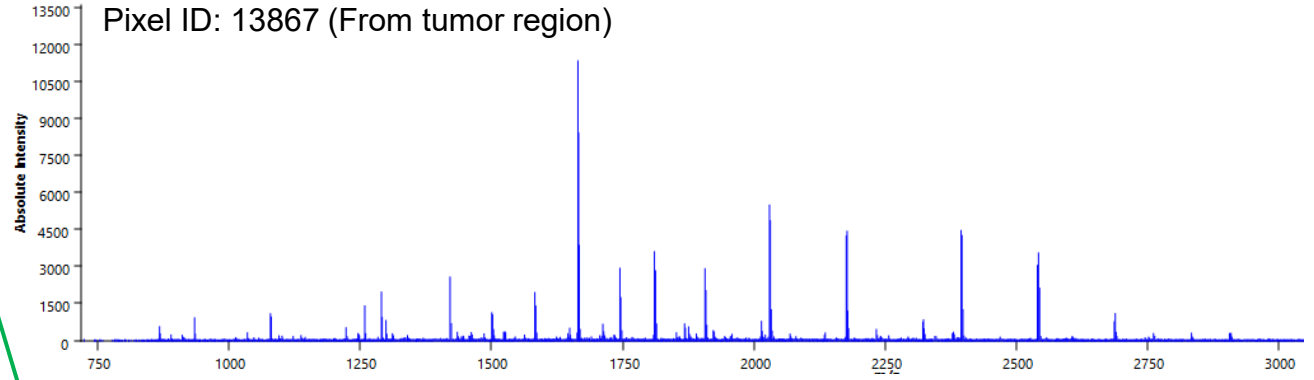


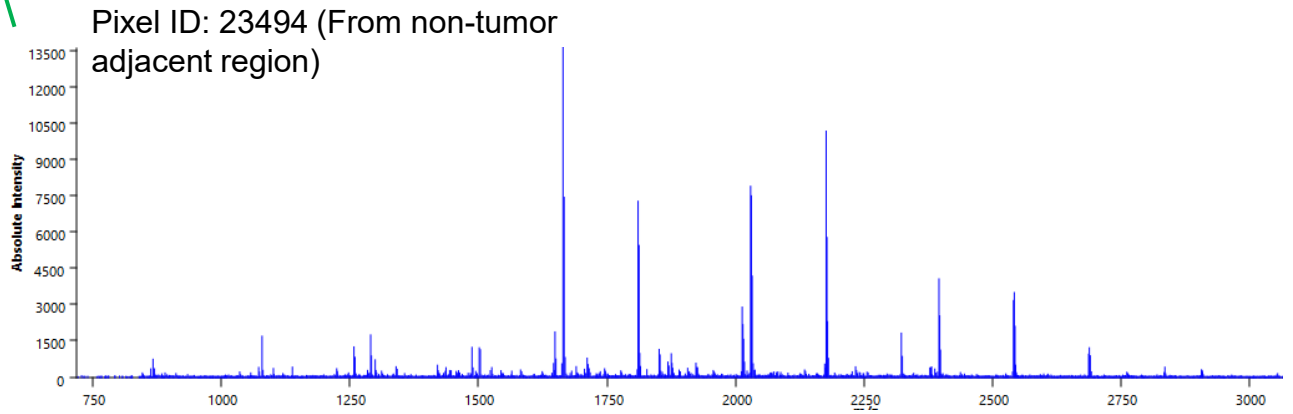
Supplemental Figure 8.

A representative sample (PT-133) demonstrating the agreement between the XGBoost-predicted tumor region (red, left) and the pathologist-annotated tumor region (black, right).



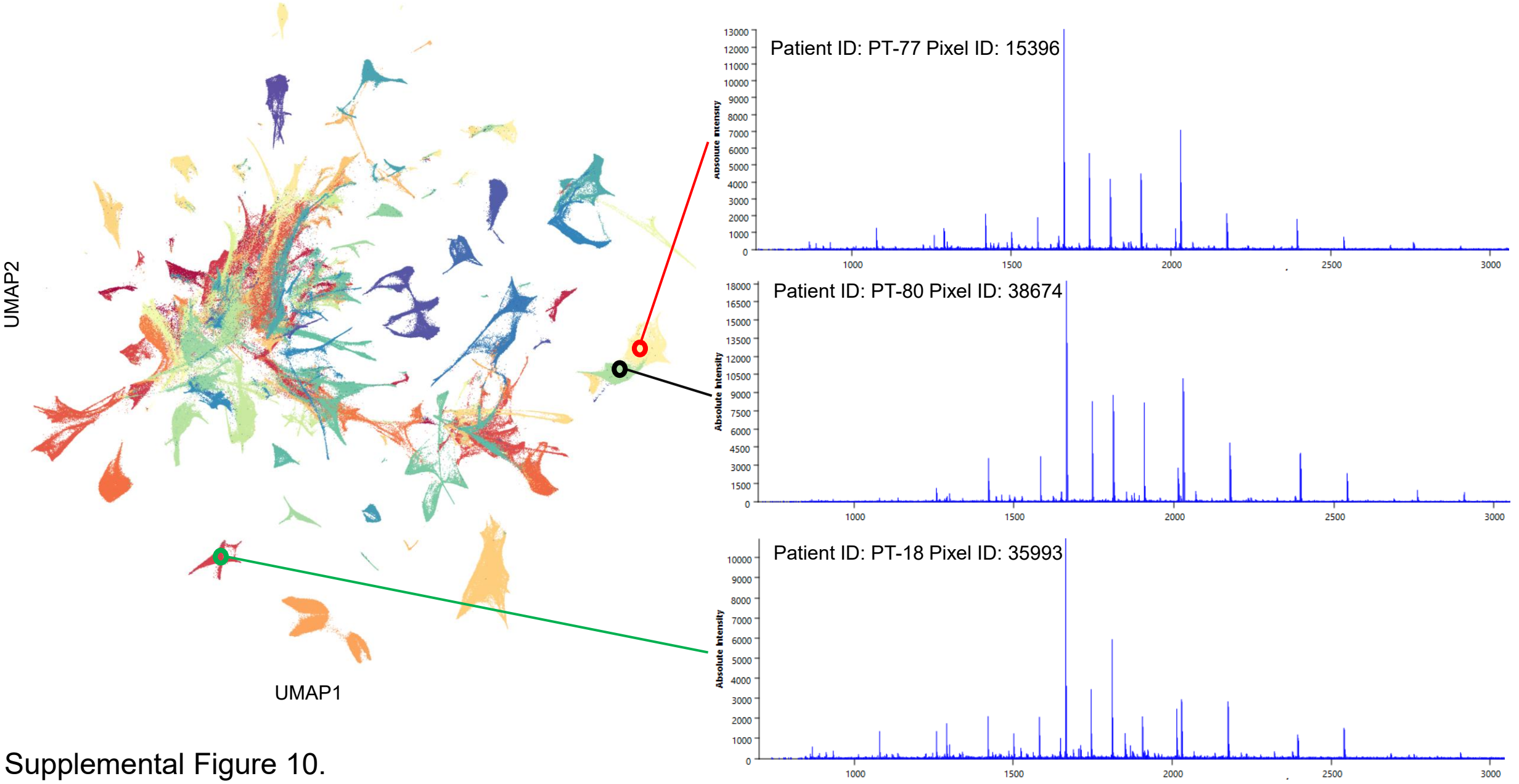






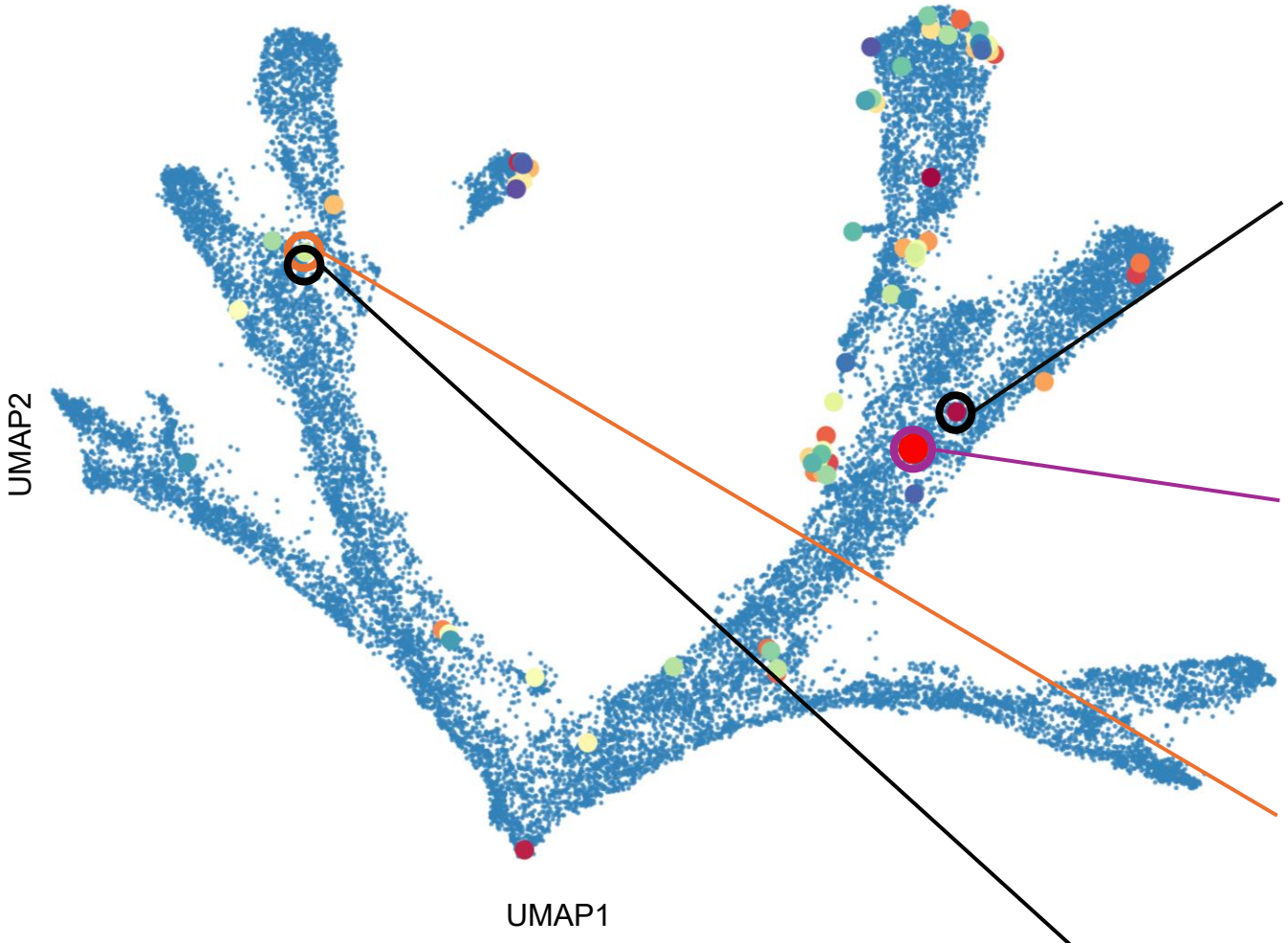
Supplemental Figure 9.

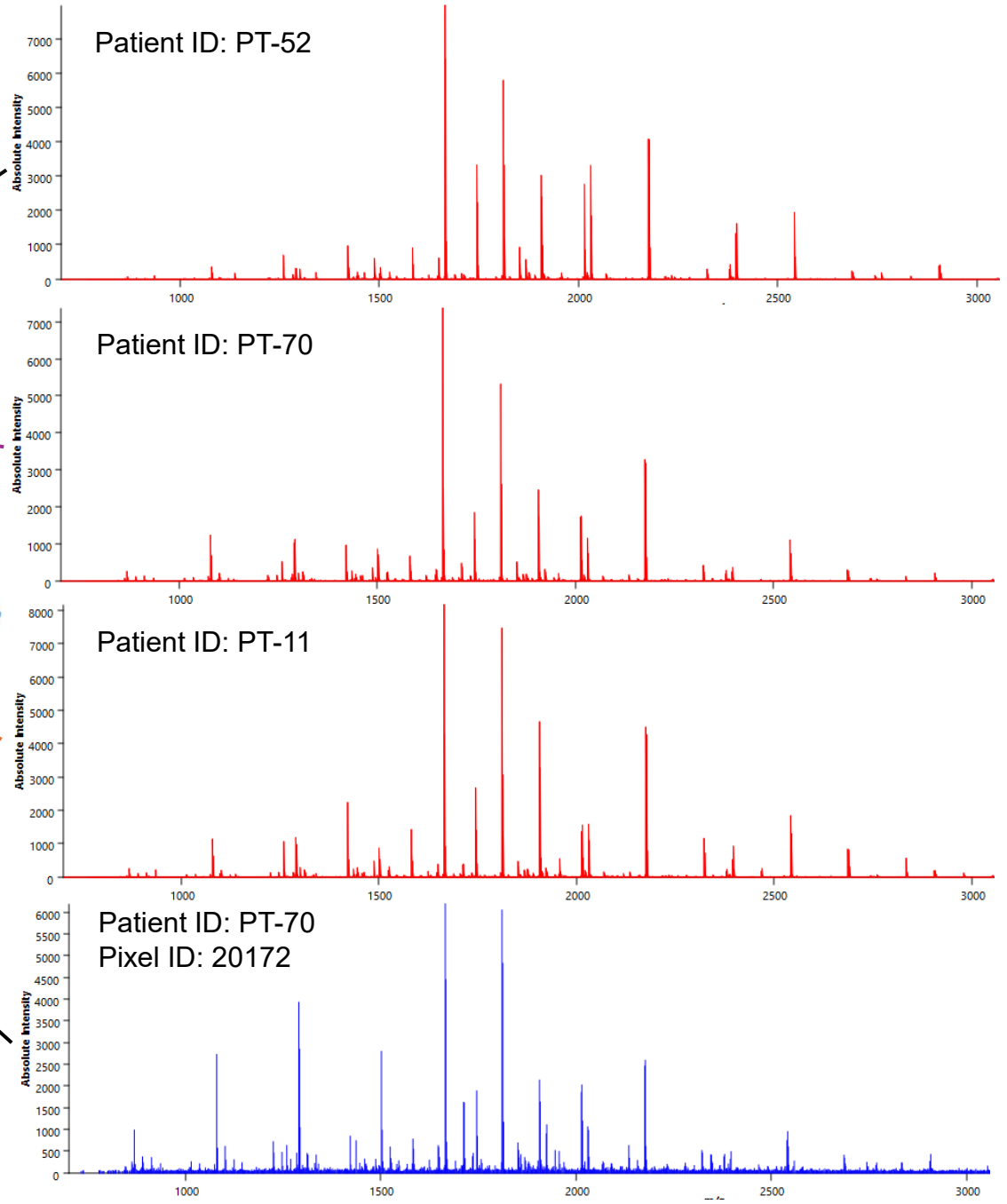
On the left, UMAP of an HCC patient (PT-59) showing distinct clustering of tumor (blue) and adjacent non-tumor (orange) regions based on glycan profiles. Each point represents a single pixel from MALDI imaging, demonstrating the ability of glycan profiles to distinguish between tumor and adjacent non-tumor tissues as annotated by a pathologist. On the right, mass spectra of selected pixels.



Supplemental Figure 10.

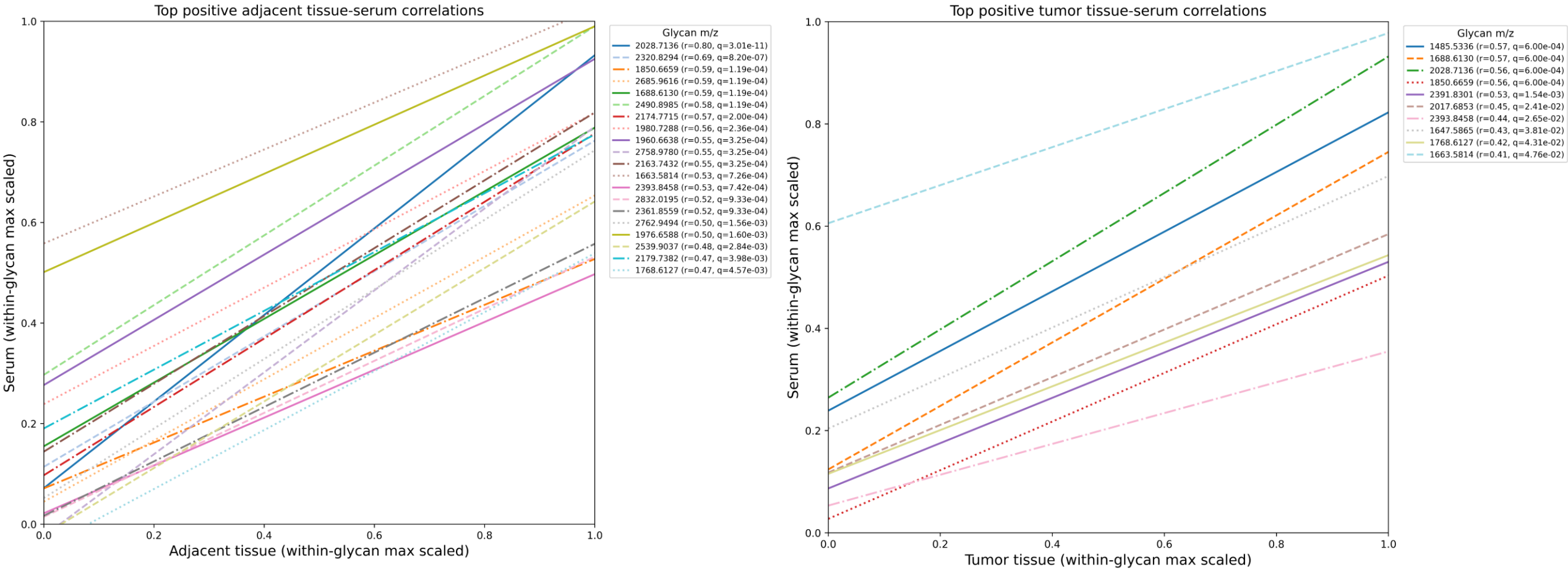
On the left, Global UMAP of tumor pixels from all patients in the cohort, demonstrating the overall heterogeneity of HCC tumors and shared glycan profiles across patients. On the right, mass spectra of selected pixels.





Supplemental Figure 11.

On the left is a representative UMAP illustrating tumor heterogeneity and inter-patient variability. The blue pixels represent individual pixels from a single patient's tumor region. Colored pixels represent the mean glycan profiles of tumor regions from other patients in the cohort. The large red pixel indicates the mean value of all tumor pixels from the patient represented by the blue pixels. On the right are the mass spectra of selected patients and a single pixel. Note that normalization is applied to the raw mass spectra as defined in the Methods section.



Supplemental Figure 12.

For patients in the discovery cohort, TIC- and total-glycan–normalized relative intensities were averaged across all pixels within the pathologist-annotated adjacent non-tumor (left) or tumor (right) region and correlated with the intensity of the same N-glycan composition in matched serum. Values were rescaled within each glycan to its cohort-wide maximum for display on common axes; this transformation is monotonic and does not affect the correlation coefficients. Lines are ordinary least-squares fits, with individual points omitted for clarity. Pearson r and Benjamini–Hochberg–adjusted q values are shown for each species. Left, the 20 most strongly positively correlated adjacent tissue–serum species. Right, all tumor tissue–serum species reaching q < 0.05. Six species were significant in both comparisons (m/z 1663.581, 1688.613, 1768.613, 1850.666, 2028.714, 2393.846), including m/z 2393.846, the strongest positive SHAP contributor to tumor classification (Figure 5D).